Research Article | Vol. 9, No. 1 | 1 Jan 2019 | OPTICAL MATERIALS EXPRESS 330
Optical Materials EXPRESS

Near-perfect absorption throughout the visible using ultra-thin metal films on index-near-zero substrates [Invited]

LISA J. KRAYER, JONGBUM KIM, AND JEREMY N. MUNDAY*

Electrical and Computer Engineering Department, University of Maryland, College Park, MD 20742, USA
**jnmunday@umd.edu*

Abstract: Metals are highly reflective and therefore commonly overlooked as efficient absorbers. However, a subwavelength Fabry-Pérot-like resonance in ultra-thin metal films has been used to achieve absorption above 70%, approaching perfect absorption using traditional substrates. Here we take a different approach and show that near-perfect absorption is achievable provided that the ultra-thin metals are deposited on an index near zero (INZ) substrate. The optical contrast at the metal-INZ interface enhances the non-trivial reflections leading to destructive interference after multiple reflections. In this manuscript, we present design considerations for ultra-thin metal films on INZ substrates to obtain near-perfect absorption throughout the visible spectrum and into the near-infrared (NIR). We find that metals commonly used for plasmonics and hot carrier devices, such as Au and Ag, can obtain near-perfect absorption for near-ultraviolet and visible wavelengths, while metals such as Pd and Pt are efficient absorbers throughout the near-ultraviolet to near-infrared spectrum.

1. Introduction

Generating optical interference in thin films is a versatile method of controlling light absorption, reflection, and transmission in materials. Such interference is responsible for the rainbow colors seen in oil on water and is incorporated into many devices for anti-reflection coatings [1,2], optical filters [2–4], thin film solar energy conversion [5], and even lasers [6–8]. Traditional interference effects use a lossless material that is a half or a quarter of the thickness of the incident wavelength within the material for constructive or destructive interference, respectively. However, it was recently shown that lossy, reflecting materials can achieve destructive interference in film thicknesses much less than the quarter wavelength requirement as a result of accumulated phase shifts upon reflection from each interface [9,10]. This resonance is a subwavelength Fabry-Pérot-like resonance and is unlike tradition Fabry-Pérot (FP) resonances because it requires the optical cavity to be both highly attenuating and 10-100x thinner than the wavelength of light to allow multiple reflections for destructive interference. This effect is unique because highly attenuating materials typically are also highly reflective and therefore are generally not considered useful as an optical cavity. This resonance has been applied to obtain high absorption in ultra-thin semiconductors on metal substrates such as silicon (Si) and germanium (Ge) on gold (Au) or silver (Ag) [10,11], but can also be applied to metals with large refractive index, such as platinum (Pt) and chromium (Cr) on dielectric substrates [12].

Significant research has gone into design considerations for the absorption resonance in thin semiconductors on metal substrates [10,11,16–20]; however, absorption resonances in planar, thin metal films has not been thoroughly investigated. Metals are more reflecting than semiconductors and are therefore commonly overlooked for efficient absorption. Rensberg *et. al.* [18] demonstrated that reflection can be suppressed in thin films when their substrates have a refractive index less than unity (i.e. $\tilde{n}_{\text{substrate}} = n_s + i\kappa_s < 1$). Low loss, index-near-zero (INZ)

#348425 https://doi.org/10.1364/OME.9.000330
Journal © 2019 Received 22 Oct 2018; revised 22 Nov 2018; accepted 24 Nov 2018; published 21 Dec 2018

Optical Materials EXPRESS

materials offer high optical contrast to most media, including air and therefore enhance the FP like resonance in the thin absorbing films. In this paper, we present design considerations for obtaining near-perfect, absorption in planar, thin metal films varying the optical properties of nearly-ideal INZ substrates and incident optical wavelengths from near-ultraviolet (NUV) to near-infrared (NIR). As expected, we find that the absorption in the metal film decreases with increasing n_s, but we find that the absorption does not significantly decrease with increasing loss (κ_s). In addition, we find that metals commonly used for plasmonics, such as Au and Ag, can be used to obtain high absorption in NUV and visible wavelengths, while lower conductive metals such as Pt and Cr have high absorption over a broader range of wavelengths from visible to NIR.

2. Absorption resonance with an ideal INZ substrate

It was previously shown that the absorption in an ultra-thin metal film can be estimated by the optical contrast of the media surrounding the film [13–15,21]. If the surrounding media are optically thick and non-absorbing, the optical path length in the film is very small (i.e. $\delta = 2\pi d/\lambda \ll 1$, where d is the film thickness and λ is the wavelength in air), and the real and imaginary parts of the thin film's refractive index are approximately equal (*i.e.* $n_f \approx \kappa_f$, where n_f and κ_f are the real and imaginary parts of the refractive index of the metal film, respectively), then the maximum absorption attainable in a thin film is determined by:

$$A_{\max} \approx \frac{n_{top}}{n_{top} + n_{bot}} \tag{1}$$

where n_{top} and n_{bot} are the real parts of the refractive indices of the media above and below the metal film respectively. From this approximation there are two methods of obtaining near-perfect absorption in a thin metal film. The first is to ensure that $n_{top} \gg n_{bot}$, and the second is to reduce n_{bot} to zero. Here, we consider this second case.

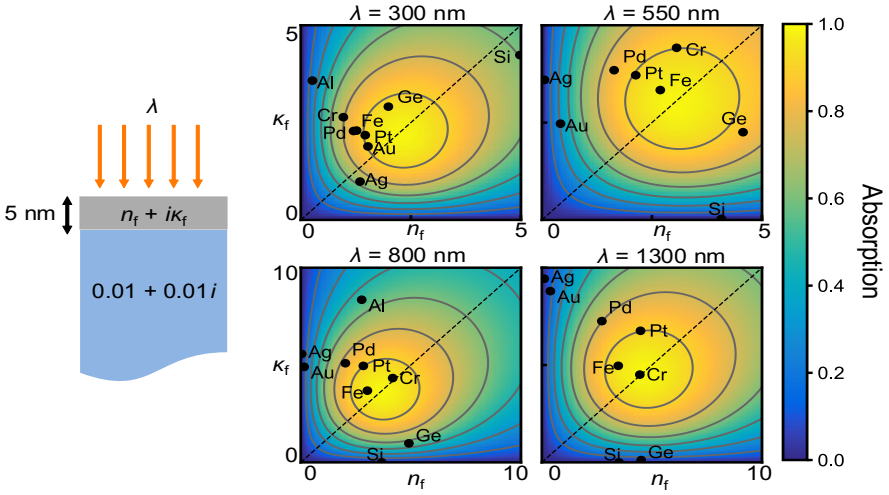

Fig. 1. Absorption resonance in a 5 nm metal film varying the refractive index, $n_f + i\kappa_f$, for wavelengths 300, 550, 800 and 1300 nm. The black dots show the optical properties of various materials. The dotted line shows $n_f = \kappa_f$. The n_f and κ_f axis extend from 0 to 5 for wavelengths 300 and 550 nm and are increased from 0 to 10 for wavelengths 800 to 1300 nm due to the increased size of the resonance. Some metals do not show up in all plots because their refractive indices lie outside of the values shown.

Optical Materials EXPRESS

Figure 1 shows the absorption resonance within the metal film at four wavelengths incident from air on a 5 nm thick film with refractive indices $n_f + i\kappa_f$ on a nearly ideal INZ substrate (*i.e.* $n_{top} = n_{air} = 1$ and $\tilde{n}_{bot} = 0.01 + 0.01i$). The absorption maximum for all wavelengths is 99%, which is correctly estimated by Eq. (1). While the value of the absorption maximum is independent of wavelength and film thickness, the optical properties of the thin films that achieve the maximum absorption is dependent on these parameters. In Fig. 1, we see that the range of n_f and κ_f values that achieve ultra-high absorption decreases and moves closer to the origin with decreasing wavelength. Note that it was previously shown that the resonance decreases in this same manner with increasing film thickness at a fixed wavelength [12,13]. The optical properties of various metals as well as Si and Ge are shown to determine what common materials will satisfy the absorption resonance. The optical properties were taken from references [22–26].

Pt and Fe remain in the absorption resonance corresponding to > 90% absorption at all wavelengths, while Pd remains just outside the resonance maxima at ~80% absorption. Cr lies in the absorption maxima for all but the shortest wavelengths, whereas Au and Ag only show high absorption for short wavelengths. At 300 nm, Ag lies outside the resonance but is close to the $n_f \approx \kappa_f$ line suggesting that it would lie at the center for the resonance for film thickness larger than 5 nm. Ge and Si are both close to the absorption resonance at 300 nm and Ge remains close to the absorption maxima at 550 nm. While Si is outside the resonance at 300 nm, it is close to the $n_f = \kappa_f$ line, suggesting that Si will lie at the center of the absorption resonance for films thinner than 5 nm. This behavior is because Si has higher loss and therefore higher dampening of the incident light compared to the other materials listed at $\lambda = 300$ nm. Therefore, to obtain multiple reflections within the film for destructive interference, the Si film must be thinner than the other materials (see Fig. 2).

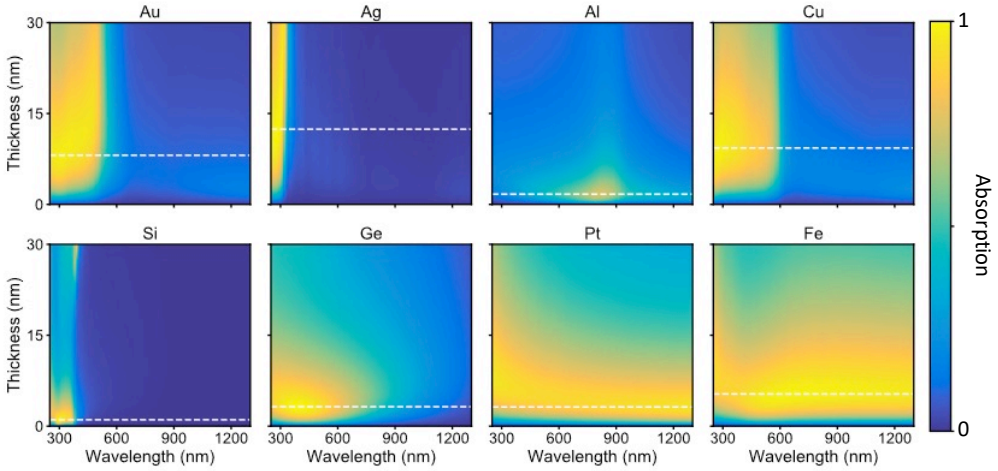

Fig. 2. Contour plots of absorption as a function of wavelength and thickness for various materials on a nearly ideal INZ substrate ($\tilde{n}_{bot} = 0.01 + 0.01i$). The white dashed lines show the thickness where the absorption is maximized in each material. Al and Si achieve maximum absorption at 1-2 nm film thicknesses. Ge and Pt achieve maximum at 3 nm. All other metals achieve maximum absorption between 5 and 15 nm film thicknesses. Pt and Fe maintain high absorption across all wavelengths.

We verify the absorption resonance on a nearly ideal INZ substrate as a function of film thickness in 8 materials in Fig. 2. As expected, Ag achieves maximum absorption at a film thickness larger than that required for Au. The maximum absorption for each material is 97% for Au, 99% for Ag, 74% for Al, 98% for Cu, 99% Si, 99% for Ge, 96% for Pt and 98% for Fe. The film thicknesses and wavelengths at maximum absorption are, respectively, 8 nm and 320

Optical Materials EXPRESS

nm for Au, 12 nm and 282 nm for Ag, 2 nm and 816 nm for Al, 9 nm and 284 nm for Cu, 1 nm and 295 nm for Si, 3 nm and 377 nm for Ge, 3 nm and 1300 nm for Pt and finally 5 nm and 653 nm for Fe.

3. Effect of non-ideal INZ optical properties

While Fig. 1 shows the absorption resonance in thin films on a nearly ideal INZ substrate, real INZ materials generally have higher optical loss because of the free carrier dampening required to obtain a low refractive index. Therefore, it is important to understand how the resonance shifts with the varied optical properties of INZ substrates with optical loss. Figure 3 shows the changes in the location and value of the absorption maxima in n_f-κ_f space varying the INZ complex refractive index, $n_{INZ} + i\kappa_{INZ}$, for three values of the effective optical path length, $\delta = 2\pi d/\lambda$. Each data point was calculated numerically using the transfer matrix method. As expected, with decreasing δ, either due to decreasing thickness or increasing wavelength, the maximum absorption occurs at larger values of n_f and κ_f.

We find that the maximum absorption is predominately determined by the real part of the INZ material's refractive index, n_{INZ}, and remains relatively constant as the optical loss, κ_{INZ}, increases for constant n_{INZ}. The absorption maxima calculated using Eq. (1) for n_{INZ} values of 0.01, 0.4 and 0.8 are 99.0%, 71.4% and 55.6%, respectively, and the exact numerically calculated values in Fig. 3 agree with these values within ± 4%. This result demonstrates that Eq. (1) can be used to estimate the value of the absorption maximum even in the presence of optical loss in the substrate. However, the values of n_f and κ_f that correspond to maximum absorption change significantly with the optical properties of the INZ substrate. As n_{INZ} increases, the maximum absorption occurs at larger values of n_f and κ_f, and as κ_{INZ} increases, the location of the absorption maximum moves away from the $n_f = \kappa_f$ line and instead requires $n_f > \kappa_f$ (Fig. 3).

As the absorption in the INZ substrate increase, *i.e.* as κ_{INZ} increases, the peak of the absorption resonance shifts to larger values of n_f and smaller values of κ_f moving the high absorption region away from the optical properties of common metals as shown in Fig. 1. However, metals that lie closer to the $n_f = \kappa_f$ line are likely to remain in the absorption resonance, provided that $\kappa_{INZ} < 1$. For example, at 300 nm incident wavelength, Au, Ag, and Pt will all remain in the absorption resonance for $\kappa_{INZ} < 1$, allowing them to obtain >90% absorption if $n_{INZ} \leq 0.11$ and their film thicknesses are optimized (i.e. d ~5nm).

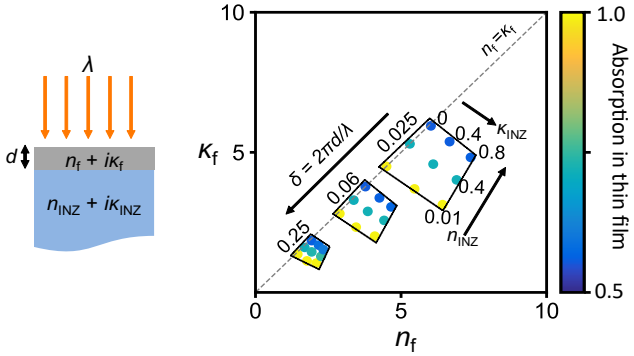

Fig. 3. Absorption maxima in thin films are shown as a function of their optical properties ($n_f + i\kappa_f$), the optical properties of the INZ substrate ($n_{INZ} + i\ \kappa_{INZ}$), and of the effective optical path length, $\delta = 2\pi d/\lambda$. The color of the dots represents the value of the absorption maxima in the thin film as determined by the color bar. The dashed grey line corresponds to $n_f = \kappa_f$. The three boxed regions represent calculated values for $\delta = 0.25$, 0.06, and 0.025 varying n_{INZ} and κ_{INZ}. The boxed region at $\delta = 0.025$ shows the values for n_{INZ} and κ_{INZ}, and this trend is consistent for all δ regions, but not shown for simplicity.

Optical Materials EXPRESS

Currently, INZ materials with the lowest refractive index reported in literature have minimum $n_{INZ} > 0.2$, and it is important to note that there is only a small optical bandwidth where both n_{INZ} and κ_{INZ} remain low [27–32]. Due to the dispersive properties of INZ materials, at short wavelengths n_{INZ} is too large for high absorption while κ_{INZ} is approximately 0. At long wavelengths, n_{INZ} will decrease, but κ_{INZ} will increase and move the absorption resonance away from all common materials. Therefore, the optical bandwidth useful for maximizing absorption in thin metal films is around the wavelength where $n_{INZ} = \kappa_{INZ}$, or $\lambda_{n=\kappa}$. INZ materials such as Al:ZnO or In:SnO have recently been of great interest because of the ability to tune $\lambda_{n=\kappa}$ by varying deposition parameters such as doping and annealing temperatures [28,30,33,34]. These materials have previously reported tunable $\lambda_{n=\kappa}$ in mid-IR wavelengths, but recently they have achieved $\lambda_{n=\kappa}$ in the NIR. For example, Kim *et al.* in ref [29] reports INZ optical properties in 2 wt% Al:ZnO with $\lambda_{n=\kappa}$ at 1290.5 nm. The optical properties at this wavelength are $n_{INZ} = \kappa_{INZ}$ ~0.39. However, n_{INZ} reaches a minimum of ~0.2 with $\kappa_{INZ} > 1$ for $\lambda > 1435$ nm. Therefore, a thin metal film deposited on this substrate would reach an absorption maximum of 70-80% absorption for a narrow bandwidth between 1290 and 1435 nm.

4. Ultra-high absorption in common thin metal films

Figures 1 and 3 show that it is necessary for the INZ substrate to have small real and imaginary parts of its refractive index to enhance absorption in common metals. There are currently no reported INZ materials in visible wavelengths; however, designing materials to have INZ behavior in this region has been a topic of considerable interest in recent years. Assuming it will be possible to find an INZ material with low refractive index that is tunable to any wavelength, it would be useful to look at which common metals will benefit from the enhanced absorption resonance. Previous results have shown that Pt, Cr, Fe and Ti obtain high absorption from 1100 – 1600 nm [12]. Here, we consider the absorption in various metals from 250 – 900 nm. Figure 4 shows the numerically calculated absorption in eight common metals on INZ substrates with nearly ideal INZ ($\tilde{n}_{bot} = 0.01 + i0.01i$) and low loss values ($\tilde{n}_{bot} = 0.25 + 0.25i$) for the optical properties assuming no dispersion in the INZ substrate. The film thicknesses are optimized at each wavelength (Fig. 4). Because dispersion prevents real INZ materials from maintaining low loss and low refractive index over this large bandwidth, Fig. 4 should be considered a reference for selecting materials with high absorption given an INZ substrate with $\lambda_{n=\kappa}$ between 250 and 900 nm. The absorption spectra for each metal on a real, dispersive INZ substrate would reach the maximum values plotted here only for a narrow bandwidth around $\lambda_{n=\kappa}$.

Because Pt, Pd and TiN remain close to the $n_f = \kappa_f$ line, these metals are useful for high absorption throughout the NUV to NIR spectrum. Note that increasing the difference between n_f and κ_f reduces the absorption in the thin film. For example, Mg will never have absorption larger than 30% because $\kappa_{Mg} \gg n_{Mg}$ at all wavelengths. Similarly, the absorption in Cr decreases for visible wavelengths where $\kappa_{Cr} > n_{Cr}$. The only metal that does not follow this trend is Al. This result is because n_{Al} becomes relatively large at ~800 nm, allowing it to lie just outside the absorption resonance for > 50% absorption, which can also be seen in Fig. 1.

When the optimized film thickness is > 30 nm, the absorption is no longer maximized by the thin film FP resonance and instead is maximized by the bulk material absorption. Note that for a glass substrate, the optimized absorption is often from the bulk rather than the thin film resonance because of the reduced optical contrast. The absorption in Ag at ~350 nm is not due to a thin film FP resonance either, because at this wavelength Ag behaves more like a dielectric instead of a metal, and n_{Ag} and κ_{Ag} are too small to lie within the thin film absorption resonance.

Optical Materials EXPRESS

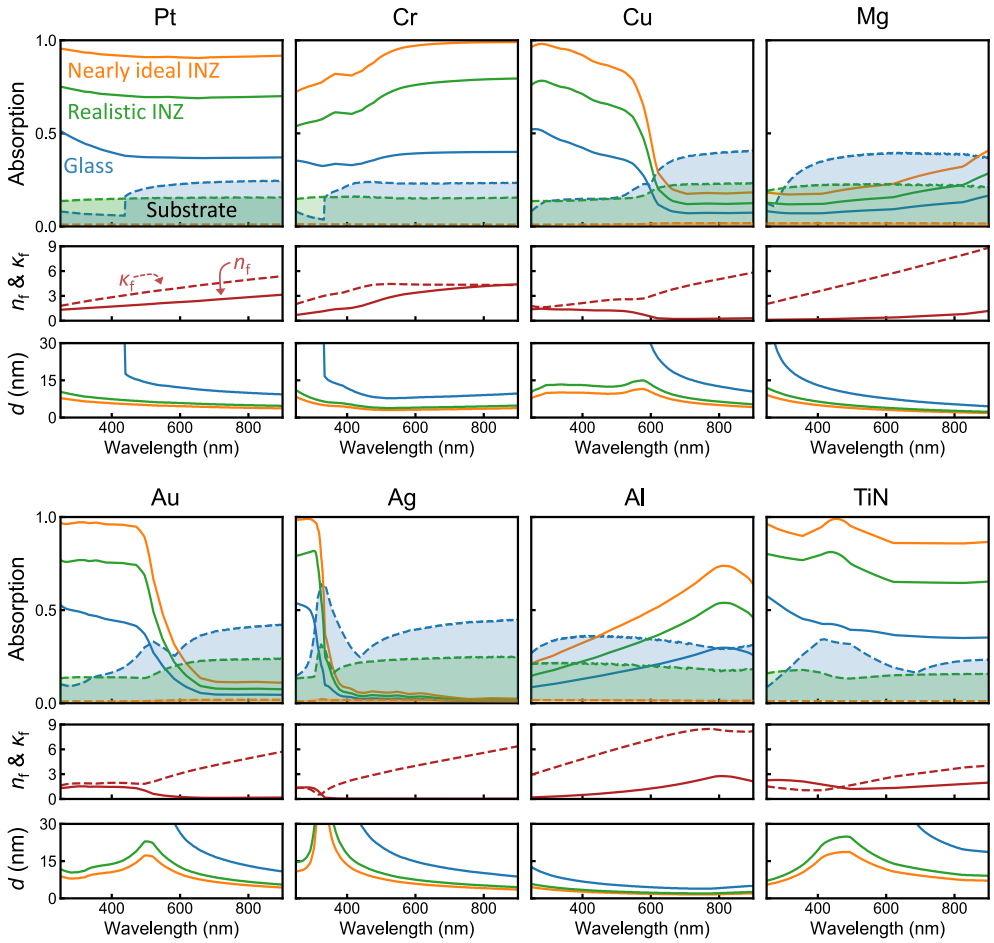

Fig. 4. Maximized absorption in various thin film metals on a nearly ideal, non-dispersive INZ substrate (orange) with $\tilde{n}_{bot} = 0.01 + 0.01i$, a low loss, non-dispersive INZ substrate (green) with $\tilde{n}_{bot} = 0.25 + 0.25i$, and a glass substrate (blue). The refractive index, n_f (solid) + $i\kappa_f$ (dashed), is plotted below the absorption. The transmission into the substrate is shown by the dashed lines and shaded regions. At each wavelength the film thickness, d, is optimized, and the optimized values are plotted.

While there is negligible transmission into the ideal INZ substrate for all metals, the maximum transmission into the lossy INZ substrate is 31% at the crossover wavelength for Ag. Because the INZ substrate is optically thick it can be assumed that all light transmitted into the substrate will eventually be absorbed. However, the BK7 glass substrate has no absorption beyond 400 nm, and therefore most of the transmitted light will eventually exit the substrate into free space. Finally, we find that illumination with TM polarized light enables near angular independence of enhanced absorption in the metal film. Figure 5 shows the absorption in Pt, Au, Al and TiN, at wavelengths and film thicknesses chosen to maximize the absorption at normal incidence, varying the incident angle and polarization of illumination. For the nearly ideal INZ substrate with $\tilde{n}_{bot} = 0.01 + 0.01i$ and the glass substrate, the absorption with TM illumination remains constant until $\theta > 60°$. Interestingly, the metals on the INZ substrate with higher refractive index, $\tilde{n}_{bot} = 0.25 + 0.25i$, increase in absorption for $\theta > 30°$ before decreasing at $\theta > 60°$. This is because the lossy INZ substrate will not have perfect reflection at the

Optical Materials EXPRESS

metal/INZ interface for normal incidence allowing some of the light to transmit into the INZ substrate. However, after the critical angle, the reflectivity at the metal/INZ substrate will increase and enhance the absorption within the thin metal film.

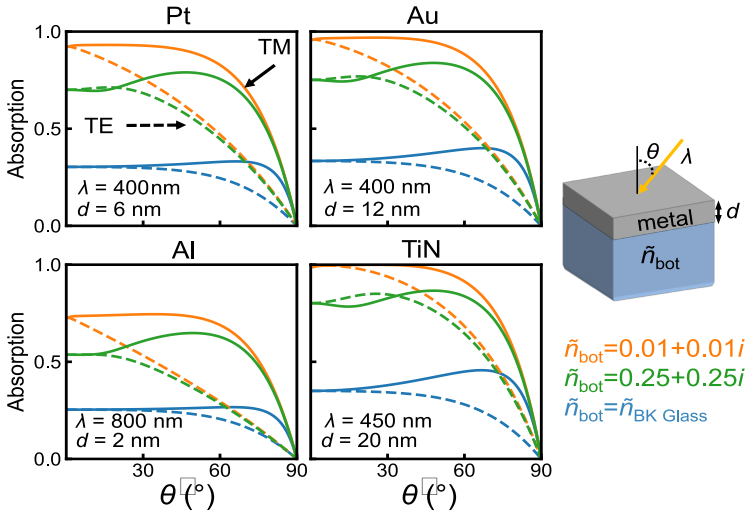

Fig. 5. Absorption in four metals varying the incident angle for TM (solid) and TE (dashed) illumination. The absorption in each metal is compared when using a glass substrate (blue), a nearly ideal INZ substrate with $\tilde{n}_{bot} = 0.01 + 0.01i$ (orange), and a low loss INZ substrate with $\tilde{n}_{bot} = 0.25 + 0.25i$ (green). The absorption is calculated numerically using the transfer matrix method with the specified parameters for wavelength, λ, and film thickness, d, denoted within the plots. The film thickness and wavelengths were chosen to maximize the absorption.

5. Conclusions

In conclusion, we have shown design consideration for obtaining nearly perfect absorption in ultra-thin metal films on INZ substrates throughout the visible spectrum. Provided that the optical loss in the INZ substrate is low, the optimum thin film will have $n_f \sim \kappa_f$. However, as the optical loss in the INZ substrate increases, an optimum thin film would have $n_f > \kappa_f$. We find that while metals such as Pt, Cr, and Fe will have high absorption for NIR wavelengths, metals that are more commonly used for hot carrier and plasmonic devices such as Au and Ag can obtain high absorption in NUV and visible wavelengths. In addition, Al films as thin as 2 nm can have > 50% absorption on an INZ substrate at wavelengths near 800 nm. Presently, it is rare to find INZ materials in the visible to NIR wavelengths. Most INZ materials have INZ properties in NUV or mid-IR wavelengths. However, recently significant research has been done to fabricate bulk INZ materials or design metamaterials that act as effective INZ substrates in this wavelength region [30,35,36]. Further opportunities exist for tailoring the properties of the thin-film metals either through alloying [37] or dynamically switching their refractive indices in the visible [38]. Future work in materials' design could enable ultra-high absorption throughout a wide spectral range for optoelectronic devices such as hot carrier detectors and energy convertors [39,40], as well as color pixels and optical filters.

Funding

This material is based upon work supported by the National Science Foundation CAREER Grant No. ECCS-1554503 and the Office of Naval Research YIP Award under Grant No. N00014-16-1-2540. L.J.K. is supported by a NSF Graduate Research Fellowship (DGE 1322106, ECCS-1554503) and an Ann G. Wylie Dissertation Fellowship.

Optical Materials EXPRESS

References

1. K.-H. Kim and Q.-H. Park, "Perfect anti-reflection from first principles," Sci. Rep. **3**(1), 1062 (2013).
2. H. Macleod, *Thin-Film Optical Filters, Third Edition* (Taylor & Francis Group, 2001).
3. Y.-J. Jen, C.-C. Lee, K.-H. Lu, C.-Y. Jheng, and Y.-J. Chen, "Fabry-Pérot based metal-dielectric multilayered filters and metamaterials," Opt. Express **23**(26), 33008–33017 (2015).
4. C. Pinheiro, J. G. Rocha, L. M. Goncalves, S. Lanceros-Mendez, and G. Minas, "A Tunable Fabry-Pérot Optical Filter for Application in Biochemical Analysis of Human's Fluids," in *2006 IEEE International Symposium on Industrial Electronics* (2006), **4**, pp. 2778–2783.
5. L. A. Weinstein, W.-C. Hsu, S. Yerci, S. V. Boriskina, and G. Chen, "Enhanced absorption of thin-film photovoltaic cells using an optical cavity," J. Opt. **17**(5), 055901 (2015).
6. S. W. Corzine, R. S. Geels, J. W. Scott, R.-H. Yan, and L. A. Coldren, "R.- Yan, and L. A. Coldren, "Design of Fabry-Pérot surface-emitting lasers with a periodic gain structure," IEEE J. Quantum Electron. **25**(6), 1513–1524 (1989).
7. Y. O. Barmenkov, D. Zalvidea, S. Torres-Peiró, J. L. Cruz, and M. V. Andrés, "Effective length of short Fabry-Pérot cavity formed by uniform fiber Bragg gratings," Opt. Express **14**(14), 6394–6399 (2006).
8. Y. Yamamoto, "Characteristics of AlGaAs Fabry-Pérot cavity type laser amplifiers," IEEE J. Quantum Electron. **16**(10), 1047–1052 (1980).
9. M. A. Kats, D. Sharma, J. Lin, P. Genevet, R. Blanchard, Z. Yang, M. M. Qazilbash, D. N. Basov, S. Ramanathan, and F. Capasso, "Ultra-thin perfect absorber employing a tunable phase change material," Appl. Phys. Lett. **101**(22), 221101 (2012).
10. M. A. Kats, R. Blanchard, P. Genevet, and F. Capasso, "Nanometre optical coatings based on strong interference effects in highly absorbing media," Nat. Mater. **12**(1), 20–24 (2013).
11. S. S. Mirshafieyan and J. Guo, "Silicon colors: spectral selective perfect light absorption in single layer silicon films on aluminum surface and its thermal tunability," Opt. Express **22**(25), 31545–31554 (2014).
12. L. J. Krayer, E. M. Tennyson, M. S. Leite, and J. N. Munday, "Near-IR Imaging Based on Hot Carrier Generation in Nanometer-Scale Optical Coatings," ACS Photonics **5**(2), 306–311 (2018).
13. C. Hägglund, S. P. Apell, and B. Kasemo, "Maximized optical absorption in ultrathin films and its application to plasmon-based two-dimensional photovoltaics," Nano Lett. **10**(8), 3135–3141 (2010).
14. E. F. C. Driessen and M. J. A. de Dood, "The perfect absorber," Appl. Phys. Lett. **94**(17), 171109 (2009).
15. E. F. C. Driessen, F. R. Braakman, E. M. Reiger, S. N. Dorenbos, V. Zwiller, and M. J. A. de Dood, "Impedance model for the polarization-dependent optical absorption of superconducting single-photon detectors," Eur. Phys. J. Appl. Phys. **47**(1), 10701 (2009).
16. J. Park, S. J. Kim, and M. L. Brongersma, "Condition for unity absorption in an ultrathin and highly lossy film in a Gires-Tournois interferometer configuration," Opt. Lett. **40**(9), 1960–1963 (2015).
17. H. Dotan, O. Kfir, E. Sharlin, O. Blank, M. Gross, I. Dumchin, G. Ankonina, and A. Rothschild, "Resonant light trapping in ultrathin films for water splitting," Nat. Mater. **12**(2), 158–164 (2013).
18. J. Rensberg, Y. Zhou, S. Richter, C. Wan, S. Zhang, P. Schöppe, R. Schmidt-Grund, S. Ramanathan, F. Capasso, M. A. Kats, and C. Ronning, "Epsilon-Near-Zero Substrate Engineering for Ultrathin-Film Perfect Absorbers," Phys. Rev. Appl. **8**(1), 014009 (2017).
19. S. S. Mirshafieyan, H. Guo, and J. Guo, "Zeroth Order Fabry–Perot Resonance Enabled Strong Light Absorption in Ultrathin Silicon Films on Different Metals and Its Application for Color Filters," IEEE Photonics J. **8**(5), 1–12 (2016).
20. M. R. S. Dias, C. Gong, Z. A. Benson, and M. S. Leite, "Lithography-Free, Omnidirectional, CMOS-Compatible AlCu Alloys for Thin-Film Superabsorbers," Adv. Opt. Mater. **6**(2), 1700830 (2018).
21. C. Hilsum, "Infrared Absorption of Thin Metal Films," J. Opt. Soc. Am. **44**(3), 188–191 (1954).
22. E. D. Palik, *Handbook of Optical Constants of Solids, I–III* (Elsevier Inc, 1998).
23. P. B. Johnson and R. W. Christy, "Optical Constants of the Noble Metals," Phys. Rev. B. **6**(12), 4370–4379 (1972).
24. A. D. Rakić, "Algorithm for the determination of intrinsic optical constants of metal films: application to aluminum," Appl. Opt. **34**(22), 4755–4767 (1995).
25. M. A. Green, "Self-consistent optical parameters of intrinsic silicon at 300K including temperature coefficients," Sol. Energy Mater. Sol. Cells **92**(11), 1305–1310 (2008).
26. A. Ciesielski, L. Skowronski, W. Pacuski, and T. Szoplik, "Permittivity of Ge, Te and Se thin films in the 200–1500 nm spectral range. Predicting the segregation effects in silver," Mater. Sci. Semicond. Process. **81**, 64–67 (2018).
27. A. Capretti, Y. Wang, N. Engheta, and L. Dal Negro, "Enhanced third-harmonic generation in Si-compatible epsilon-near-zero indium tin oxide nanolayers," Opt. Lett. **40**(7), 1500–1503 (2015).
28. C. Chen, Z. Wang, K. Wu, and H. Ye, "Tunable near-infrared epsilon-near-zero and plasmonic properties of Ag-ITO co-sputtered composite films," Sci. Technol. Adv. Mater. **19**(1), 174–184 (2018).
29. J. Kim, G. V. Naik, N. K. Emani, U. Guler, and A. Boltasseva, "Plasmonic Resonances in Nanostructured Transparent Conducting Oxide Films," IEEE J. Sel. Top. Quantum Electron. **19**(3), 4601907 (2013).
30. J. Kim, G. V. Naik, A. V. Gavrilenko, K. Dondapati, V. I. Gavrilenko, S. M. Prokes, O. J. Glembocki, V. M. Shalaev, and A. Boltasseva, "Optical Properties of Gallium-Doped Zinc Oxide—A Low-Loss Plasmonic Material: First-Principles Theory and Experiment," Phys. Rev. X **3**(4), 041037 (2013).

Optical Materials EXPRESS

31. J. Kim, A. Dutta, G. V. Naik, A. J. Giles, F. J. Bezares, C. T. Ellis, J. G. Tischler, A. M. Mahmoud, H. Caglayan, O. J. Glembocki, A. V. Kildishev, J. D. Caldwell, A. Boltasseva, and N. Engheta, "Role of epsilon-near-zero substrates in the optical response of plasmonic antennas," Optica **3**(3), 339 (2016).
32. M. Z. Alam, I. De Leon, and R. W. Boyd, "Large optical nonlinearity of indium tin oxide in its epsilon-near-zero region," Science **352**(6287), 795–797 (2016).
33. Y. Wang, A. C. Overvig, S. Shrestha, R. Zhang, R. Wang, N. Yu, and L. Dal Negro, "Tunability of indium tin oxide materials for mid-infrared plasmonics applications," Opt. Mater. Express **7**(8), 2727 (2017).
34. J. Yoon, M. Zhou, M. A. Badsha, T. Y. Kim, Y. C. Jun, and C. K. Hwangbo, "Broadband Epsilon-Near-Zero Perfect Absorption in the Near-Infrared," Sci. Rep. **5**(1), 12788 (2015).
35. W. D. Newman, C. L. Cortes, J. Atkinson, S. Pramanik, R. G. DeCorby, and Z. Jacob, "Ferrell–Berreman Modes in Plasmonic Epsilon-near-Zero Media," ACS Photonics **2**(1), 2–7 (2015).
36. E. J. R. Vesseur, T. Coenen, H. Caglayan, N. Engheta, and A. Polman, "Experimental verification of n = 0 structures for visible light," Phys. Rev. Lett. **110**(1), 013902 (2013).
37. C. Gong and M. S. Leite, "Noble Metal Alloys for Plasmonics," ACS Photonics **3**(4), 507–513 (2016).
38. K. J. Palm, J. B. Murray, T. C. Narayan, and J. N. Munday, "Dynamic Optical Properties of Metal Hydrides," ACS Photonics **5**(11), 4677–4686 (2018).
39. T. Gong and J. N. Munday, "Materials for hot carrier plasmonics," Opt. Mater. Express **5**(11), 2501 (2015).
40. T. Gong and J. N. Munday, "Angle-independent hot carrier generation and collection using transparent conducting oxides," Nano Lett. **15**(1), 147–152 (2015).